JOURNAL OF THERMOPHYSICS AND HEAT TRANSFER
Vol. 18, No. 2, April–June 2004

# Parameter Estimation in a Two-Layer Planar Gray Participating Medium

V. Swaminathan,* C. Balaji,† and S. P. Venkateshan‡
*Indian Institute of Technology Madras, Chennai 600 036, India*

**An inverse analysis is reported for simultaneous estimation of absorption and scattering coefficients for an inhomogeneous plane-parallel anisotropically scattering participating medium between isothermal, diffuse parallel plates from the knowledge of known temperature profile. A finite volume method is used to discretize the equation governing radiative heat transfer through the participating medium, and the inverse problem is solved through the minimization of the sum of square of residuals between the calculated and observed temperatures, utilizing the conjugate gradient method. The calculations are carried out for homogeneous and inhomogeneous media, and the effects of measurement errors on the accuracy of the estimated parameters are investigated.**

## Nomenclature

| | | |
|---|---|---|
| $A$ | = | area, $m^2$ |
| $\boldsymbol{c}, \boldsymbol{d}$ | = | gradient vector |
| $I$ | = | radiation intensity, $Wm^{-2}sr^{-1}$ |
| $\bar{I}$ | = | in-scattering term, $Wm^{-2}sr^{-1}$ |
| $J$ | = | objective function |
| $L$ | = | characteristic length of the domain ($L1 + L2$), m |
| $L1$ | = | thickness of the top layer of the participating medium, m |
| $L2$ | = | thickness of the bottom layer of the participating medium, m |
| $M$ | = | number of directions in $\gamma$ direction |
| $m$ | = | location from the reference $z$ axis |
| $mp$ | = | total number of measured points |
| $N$ | = | number of control volumes |
| $\boldsymbol{n}$ | = | unit vector normal to a control volume surface |
| $\boldsymbol{P}$ | = | parameter vector |
| $q$ | = | total heat transfer rate per unit width from the hot wall, $W \cdot m^{-1}$ |
| $q^*$ | = | dimensionless heat flux |
| $R$ | = | $(\kappa I_b + \sigma_s \bar{I})/\beta$, $W \cdot m^{-2} \cdot Sr^{-1}$ |
| $\Re$ | = | random number |
| $\boldsymbol{r}$ | = | position vector |
| $S$ | = | distance between interpolation point $uf$ and integration point $f$, m |
| $s$ | = | coordinate along path of radiation, m |
| $\boldsymbol{s}$ | = | unit vector in the direction for which $I$ is to be calculated |
| $\boldsymbol{s}'$ | = | unit vector in the center of discrete solid angle $\omega^l$ |
| $\vec{\boldsymbol{s}}$ | = | unit direction vector |
| $T$ | = | absolute temperature, K |
| $T^*$ | = | measured temperature, K |
| $v$ | = | elemental volume |
| $\alpha$ | = | assumed constant |
| $\beta$ | = | extinction coefficient, $m^{-1}$ |
| $\gamma$ | = | polar angle, rad |
| $\Delta z$ | = | control volume thickness, m |
| $\varepsilon$ | = | emissivity of the surface |
| $\Theta$ | = | scattering angle from forward direction, rad |
| $\kappa$ | = | absorption coefficient, $m^{-1}$ |
| $\sigma$ | = | Stefan–Boltzmann constant, $5.67 \times 10^{-8}\ W \cdot m^{-2} \cdot K^{-4}$ |
| $\sigma_s$ | = | scattering coefficient, $m^{-1}$ |
| $\tau$ | = | optical thickness, $\kappa L$ |
| $\Phi$ | = | phase function for scattering |
| $\phi$ | = | azimuthal angle, rad |
| $\omega$ | = | solid angle, sr |

*Subscripts*

| | | |
|---|---|---|
| $a$ | = | average |
| $b$ | = | blackbody intensity |
| bl | = | bottom layer |
| $c$ | = | cold surface |
| $f$ | = | integration point |
| $h$ | = | hot surface |
| $n, s$ | = | north, south face of the control volume |
| $P, N, S$ | = | labels for nodes within control volumes |
| $r$ | = | radiative |
| tl | = | top layer |
| $uf$ | = | interpolation point |
| $z$ | = | $z$ direction |

*Superscripts*

| | | |
|---|---|---|
| $k$ | = | iteration count |
| $l$ | = | corresponding to direction |

## Introduction

INVERSE radiation problems in a participating medium have numerous engineering applications, for example, the determination of the radiative properties of the medium in a furnace or the atmosphere. An excellent review of the literature pertaining to thermal radiation in participating media, the methods presently used for solving this class of problems, and these methods' strengths and limitations, are discussed by Howell.[1] Inverse radiation problems have been extensively reviewed in a series of papers by McCormick.[2–4] Ho and Ozisik[5] have reported a parameter estimation method based on the inverse radiation problem for determining single scattering albedo and optical thickness from the exit intensities of an isotropically scattering slab of finite thickness. An inverse problem that deals with the prediction of the temperature distribution in a medium from the data of the radiation intensities exiting the boundaries was reported by many researchers.[6–11] Liu[12] considered the inverse radiation problem of simultaneous estimation of the temperature profile and the absorption coefficient for a nonscattering

Received 17 February 2003; revision received 1 August 2003; accepted for publication 5 September 2003. 

*Research Scholar, Heat Transfer and Thermal Power Laboratory, Department of Mechanical Engineering.

†Assistant Professor, Heat Transfer and Thermal Power Laboratory, Department of Mechanical Engineering; balaji@iitm.ac.in.

‡Professor, Heat Transfer and Thermal Power Laboratory, Department of Mechanical Engineering.

gray, one-dimensional semitransparent slab with transparent boundaries, based on knowledge of the exit radiation intensities. Park and Yoon[13] presented an inverse radiation analysis for estimating radiative parameters from temperature measurement in a three-dimensional participating media, where radiation and conduction occur simultaneously.

From the review of the literature for the class of problem presented, it can be seen that studies on parameter estimation for multilayered emitting, absorbing, and scattering media are scarce. The question of uniqueness of the estimated values of the parameters for such a problem is of fundamental interest, such as in problems like the retrieval of geophysical parameters from data obtained through remote sensing satellites.

The inverse radiation problem considered in this paper is concerned with the estimation of absorption and scattering coefficients for a two-layer gray participating medium trapped between two parallel, isothermal, infinite diffuse plates, in which each layer has different absorbing–emitting and scattering characteristics. With the finite volume method proposed by Raithby and Chui,[14] the governing equation, namely, the equation of radiative transfer, is solved to obtain the temperature profile; this is traditionally known as the forward model. The inverse problem is formulated as an optimization problem that minimizes the least-square discrepancy between the measured and the calculated temperature profiles and is solved by use of the conjugate gradient method.

## Physical Model

As shown in Fig. 1a, the geometry consists of two parallel, diffuse, isothermal, infinitely long plates separated by two different absorbing–emitting and scattering layers of a gray participating medium that is in radiative equilibrium. The top and bottom plates are at temperatures $T_c$ and $T_h$, respectively, and are separated by a distance $L$. Both of the plates have an emissivity $\varepsilon$. The one-dimensional domain is divided into $N_z$ control volumes of length $\Delta z$ in the $z$ direction, as shown in Fig. 1b. The solid angle of $4\pi$ is

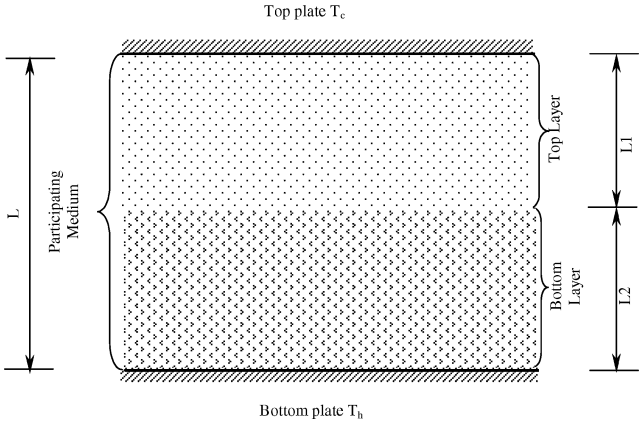


**Fig. 1a Schematic of the physical model.**

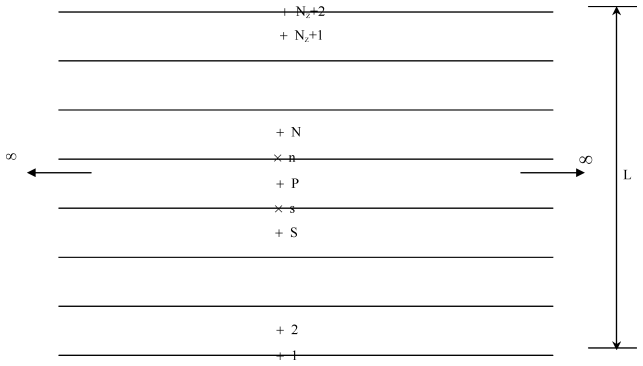


**Fig. 1b Schematic of the one-dimensional domain with control volumes.**

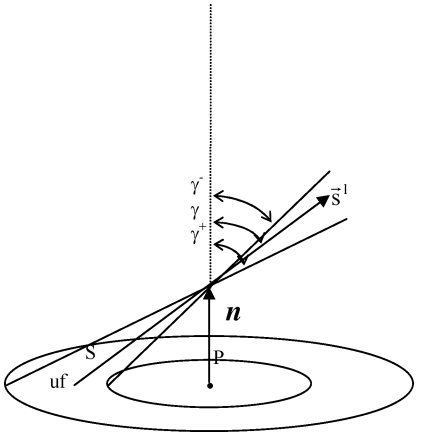


**Fig. 1c Typical solid angle.**

subdivided into conical solid angle elements ($\gamma^-$, $\gamma^+$) as shown in Fig. 1c. The direction, also an independent variable, is subdivided into $M$ solid angles, where $M$ represents the number of directions in the total polar angle $\gamma$ of $\pi$ radians. In this case, because of symmetry, the intensity is a function of $z$ and $\gamma$ only, that is, for a given ($z$, $\gamma$), the intensity is same for all azimuthal angle $\phi$ from 0 to $2\pi$.

### Direct Problem

The direct problem of concern here is to find the temperature distribution across a participating medium that is in radiative equilibrium with the plane walls. The equations governing heat transfer in a radiatively participating medium are the equation of energy and the radiation transfer equation. For the case of radiation equilibrium, the energy equation reduces to

$$\nabla \cdot q_r = 0 \tag{1}$$

where $\nabla \cdot q_r$ represents the net radiation transfer leaving the control volume in all directions. Integrating Eq. (1) over the control volume $v_P$ yields

$$-4\pi\kappa I_a v_P + 4\pi\kappa I_b v_P = 0 \tag{2}$$

that is,

$$I_a = I_b \tag{3}$$

where $I_a$ is the average intensity, given by

$$I_a = \frac{1}{4\pi}\sum_l I^l \omega^l \tag{4}$$

and $I_b = \sigma T^4/\pi$ is the average blackbody intensity corresponding to the temperature of the control volume. The average intensity in Eq. (4) has been obtained as the weighted average of the intensity within discrete solid-angle elements having solid angles of $\omega^l$. Hence, the temperature distribution of the domain can be found from Eq. (3) after solution of the radiation transfer equation.

The equation of radiation transfer, describing the change of intensity over the path length for an absorbing, emitting, and scattering medium can be written as[14,15]

$$\frac{\mathrm{d}I}{\mathrm{d}s} = -(\kappa + \sigma_s)I + (\kappa I_b + \sigma_s \bar{I}) \tag{5}$$

The left-hand side represents the rate of change of intensity. The first term on the right-hand side is the attenuation through absorption and out-scattering, and the second term is augmentation due to emission and in-scattering. Pursuant on a gray approximation for the medium, the absorption coefficient $\kappa$ and scattering coefficient $\sigma_s$ are wavelength-averaged quantities. The in-scattering term is given by[14,15]

$$\bar{I}(r, s) = \frac{1}{4\pi}\int_{4\pi} I(\boldsymbol{r}, \boldsymbol{s}')\Phi(\boldsymbol{s}', \boldsymbol{s})\,\mathrm{d}\omega' \tag{6}$$

where $I(\boldsymbol{r}, \boldsymbol{s}')$ is the intensity at $\boldsymbol{r}$ within the solid angle $\mathrm{d}\omega'$ that lies in the direction of the unit vector $\boldsymbol{s}'$. In the case of Rayleigh scattering, the phase function is given by

$$\Phi = \tfrac{3}{4}(1 + \cos^2 \Theta) \tag{7}$$

For the case of scattering of unpolarized incident radiation from a small sphere with refractive index tending to infinity, the phase function is given by[15]

$$\Phi = \tfrac{3}{5}\left[\left(1 - \tfrac{1}{2}\cos\Theta\right)^2 + \left(\cos\Theta - \tfrac{1}{2}\right)^2\right] \tag{8}$$

where $\Theta = \pi - 2\gamma$. The preceding two different cases of phase function were only considered for testing of this procedure and will be referred to subsequently as mode1 and mode 2 of scattering respectively. Equation (5) is integrated over the control volume $v_p$ and $\omega^l$. By application of the Gauss divergence theorem, the volume integral on the left-hand side of Eq. (5) is converted into a surface integral. Approximating all of the variables on the right-hand side to be constant at the nodal value while carrying out the volume integration, we get

$$\sum_{f=1}^{\text{number of control faces}} A_f \int_{\omega^l} I_f(\vec{\boldsymbol{s}} \cdot \boldsymbol{n}_f)\, \mathrm{d}\omega$$

$$= \left[-(\kappa_P + \sigma_{sP})I_P^l + \kappa_P I_{bP}^l + \sigma_{sP}\bar{I}^l\right] v_P \omega^l \tag{9}$$

where the control volume is divided into two control panels $n$ and $s$. $A_f$ represents the surface area of each control panel. The intensity and the unit normal to the surface have been approximated by their values at the integration point $f$, located centrally on each control panel.

Here, $I_f$ is determined by the use of a relationship between $I_f$ and the nodal point values $I_N$ and $I_S$, and this is similar to that proposed by Raithby and Chui.[14] The value of $I_f$ is found by tracing back along the path taken by the ray in reaching $f$ along the $-\vec{\boldsymbol{s}}$ direction until a location is reached at which the intensity can be obtained by interpolation between the nodal values. The interpolation point is designated as $uf$. The integration of Eq. (5) over a path length $S$ is performed to estimate the value of $I_f$ in terms of $I_{uf}$, and the details are available in Ref. 14. Hence,

$$I_f = I_{uf} e^{-\beta_f S} + R_f(1 - e^{-\beta_f S}) - \left\{\left(\frac{\partial R}{\partial s}\right)_f \left[1 - e^{-\beta_f S}(1 + \beta_f S)\right]\right\} \Big/ \beta_f \tag{10}$$

where $\beta = \kappa + \sigma_s$ (and is called the extinction coefficient) and $R = (\kappa I_b + \sigma_s \bar{I})/\beta$. Substitution of Eq. (10) into (9) results in the expression of heat transfer across all of the control panels within $\omega^l$ in terms of $I_{uf}$ and $R_f$. The value of $R_f$ is obtained by linear interpolation by the use of the values of $R_{f,N}$ and $R_{f,S}$. In Eq. (10), the interpolation of $I_{uf}$ in terms of nodal values is also performed to obtain an expression for $I_P$ in terms of the intensity of neighboring nodal values.

#### Inverse Problem

For the inverse problem, the absorption and scattering coefficients for both the top and bottom layers of participating media are unknown, but the measured temperature profiles at a set of discrete points are available. The problem can be solved by minimization of the objective function $J$, which is expressed by the sum of square of residuals between the calculated and measured temperature, as follows:

$$J(P) = \sum_{m=1}^{mp} \left[T_{(m;P)} - T_{(m)}^*\right]^2 \tag{11}$$

where $T_{(m;P)}$ is the calculated temperature at the location $m$ with the radiative parameters $\boldsymbol{P} = (\kappa, \sigma_s)_{\text{tl}}$ when $m$ represents the top layer or $\boldsymbol{P} = (\kappa, \sigma_s)_{\text{bl}}$ when $m$ represents the bottom layer. $T_{(m)}^*$ is the measured temperature at the same location. The minimization procedure is performed with a conjugate gradient method,[16] which is widely used for problems of this kind.

## Solution Procedure

#### Direct Problem

The equation of radiation transfer is solved to obtain the intensity at each node $P$, under an initial assumption of the values of $R$ and the intensities at the bottom surface. The intensities are calculated explicitly in all directions by sweeping the domain twice, first upward and then downward. The cycle is repeated until the change in the dimensionless net heat flux at both the surfaces is less than 0.001% between successive updates of $R$. The temperature distribution is determined by the use of Eq. (3).

#### Inverse Problem

Before estimating the parameters of a system, we need experimental measurements from the system. However, for this study, we solved the direct problem with known parameters to obtain the numerical solutions and then used these numerical solutions as experimental measurements, with or without adding small random perturbations. The effect of measurement errors are taken into account with these small random perturbations, as in the following equation:

$$T_{\text{measured}}(= T^*) = T_{\text{exact}} + \Re \tag{12}$$

where $\Re$ is a random number between $\pm 5.0$. In the range of temperature considered in this study, this translates to an error of 0.87–1.34%. Once the experimental values of temperature profiles are simulated, the method proceeds under an initial assumption of some values for the absorption and scattering coefficients for the two layers of participating medium and then obtaining the temperature profile by solving the direct problem. The sum of square residuals between the calculated and measured temperatures is then obtained with Eq. (11). First, the iteration counter is set to $k = 0$, and then the following steps are taken:

1) The following gradient vector determines the variation of the objective function [Eq. (11)] with respect to the parameter vector $P$:

$$\boldsymbol{d}^{(0)} = -\left(\frac{\partial J}{\partial P}\right)^{(0)} = -\left(\frac{\partial J}{\partial \kappa_1}, \frac{\partial J}{\partial \sigma_{s1}}, \frac{\partial J}{\partial \kappa_2}, \frac{\partial J}{\partial \sigma_{s2}}\right)^{(0)} \tag{13}$$

where $P = (\kappa_1, \sigma_{s1}, \kappa_2, \sigma_{s2})$ where $\kappa_1$, $\sigma_{s1}$, $\kappa_2$, and $\sigma_{s2}$ represent the absorption and scattering coefficients of the bottom and the top layer of the participating medium, respectively. If the magnitude of the gradient vector $|\boldsymbol{d}|$ is less than 0.001, then the search stops. Otherwise, we go to step 4. (Step 1 of the conjugate gradient and the steepest descent methods are essentially the same.)

2) The gradient of the cost function is computed as

$$c^{(k)} = \left(\frac{\partial J}{\partial P}\right)^{(k)} \tag{14}$$

The modulus of the gradient of the cost function $c^{(k)}$ is calculated, and if it is less than 0.001, then the algorithm is stopped, otherwise, it continues.

3) The new conjugate direction is obtained as

$$\boldsymbol{d}^{(k)} = -c^{(k)} + \delta_k \boldsymbol{d}^{(k-1)} \tag{15}$$

where

$$\delta_k = \left(\frac{\|c^{(k)}\|}{\|c^{(k-1)}\|}\right)^2$$

4) A constant $\alpha_k = \alpha$ is assumed, such that $J(P^{(k)} + \alpha \boldsymbol{d}^{(k)})$ is minimized.

5) The parameters are changed, so that $P^{(k+1)} = P^{(k)} + \alpha \boldsymbol{d}^{(k)}$. Set $k = k + 1$, and go to step 2. The preceding steps are continued till the modulus of the gradient $c^{(k)}$ is less than 0.001.

## Results and Discussion

### Grid Independence Study

The effect of grid size ($N_z \times M$) on the solution was studied to fix the optimum number of control volumes and the number of directions. Figures 2a and 2b show the variation with respect to change in number of directions, keeping $N_z = 10$. The conditions used in Figs. 2a and 2b are given in Table 1. The emissivity of both of the plates is 1. It is clear that the percentage increase in standard deviation of the temperature profile, with respect to the temperature profile obtained with the number of directions being 22, to the change in number of directions, varies asymptotically, and the variation gets negligible when $M$ approaches 42. Consequently, the number of directions was fixed as 42.

Now, with $M = 42$, variations with respect to control volumes are studied, and these are shown in Figs. 2c and 2d. The conditions used in Figs. 2c and 2d are given in Table 1. They show the variations in the percentage increase between successive nondimensional heat fluxes with the number of control volumes used. The variations in the percentage increase of heat flux is considered negligible if it is less than 0.05%, and so 0.05% was taken as a limit to fix the number of control volumes used. By close inspection of all of the test cases shown in Figs. 2c and 2d, the number of control volumes in general was fixed as 50. In the aforementioned case, the number of control volumes used for both the layers is equal.

To check whether an increase or decrease in the ratio of control volume thicknesses of the bottom and the top layer helps us in reducing the total number of control volumes used without compromising accuracy, the following test cases given in Table 2 are examined, and the results are shown in Fig. 3. Figure 3 shows that the percentage change in the values of heat flux is negligible with the changes in the ratio of control volume thicknesses for a wide range of total number of control volumes used, and this does not help us in reducing the total number of control volumes used. For all test cases, the top and bottom wall temperatures are kept fixed at $T_c = 373$ K and $T_h = 573$ K, respectively, and the thickness of both the top and bottom layers of the participating medium are equal to 0.5 m.

**Table 1 Test conditions used for fixing number of directions and control volumes (Figs. 2a and 2b)**

| | Bottom layer | | Top layer | |
|---|---|---|---|---|
| Curve | $\kappa$, m$^{-1}$ | $\sigma_s$, m$^{-1}$ | $\kappa$, m$^{-1}$ | $\sigma_s$, m$^{-1}$ |
| | *Mode 1 scattering* | | | |
| 1 | 0.5 | 1.5 | 1.5 | 0.5 |
| 2 | 1.5 | 0.5 | 0.5 | 1.5 |
| 3 | 1.0 | 0.2 | 2.0 | 0.5 |
| 4 | 3.0 | 0.1 | 0.1 | 2.0 |
| | *Mode 2 scattering* | | | |
| 5 | 0.5 | 1.5 | 1.5 | 0.5 |
| 6 | 1.5 | 0.5 | 0.5 | 1.5 |
| 7 | 1.0 | 0.2 | 2.0 | 0.5 |
| 8 | 3.0 | 0.1 | 0.1 | 2.0 |

**Table 2 Test conditions used to fix control volume thickness for the bottom and top layers of the participating medium (Fig. 3)**

| | Number of | Bottom layer | | Top layer | |
|---|---|---|---|---|---|
| Curve | control volumes | $\kappa$, m$^{-1}$ | $\sigma_s$, m$^{-1}$ | $\kappa$, m$^{-1}$ | $\sigma_s$, m$^{-1}$ |
| | | *Mode 2 scattering* | | | |
| 1 | 36 | 3.0 | 0.2 | 0.5 | 0.2 |
| 2 | 28 | 3.0 | 0.2 | 0.5 | 0.2 |
| 3 | 46 | 5.0 | 0.2 | 1.0 | 0.2 |
| 4 | 110 | 5.0 | 0.2 | 1.0 | 0.2 |
| 5 | 110 | 3.0 | 0.2 | 0.5 | 0.2 |
| | | *Mode 1 scattering* | | | |
| 6 | 110 | 3.0 | 0.2 | 0.5 | 0.2 |
| 7 | 110 | 5.0 | 0.2 | 1.0 | 0.2 |

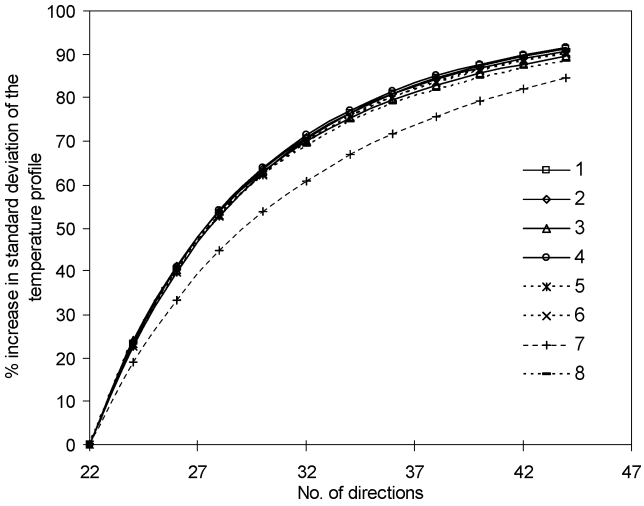


**Fig. 2a Variation of percent increase in standard deviation of the temperature profile with respect to a profile obtained with the number of direction being 22; conditions used for generating curves are given in Table 1.**

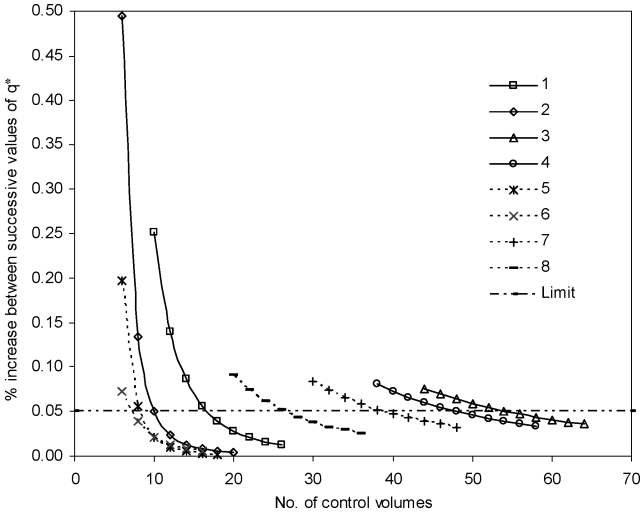


**Fig. 2b Variation of percent increase between successive nondimensional heat fluxes with the number of control volumes; conditions used for generating curves are given in Table 1.**

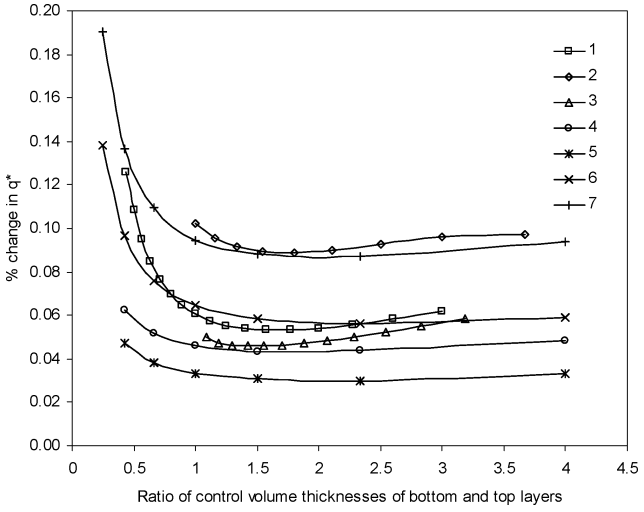


**Fig. 3 Variation of percent change in nondimensional heat fluxes with respect to their mean value, with the ratio of control volume thickness between two layers of participating medium; conditions used for generating curves are given in Table 2.**

**Table 3 Dimensionless heat flux for the case of radiative equilibrium between two isothermal, diffuse, infinitely long parallel plates**

| Optical thickness $\tau$ | $q^*$(present), $4 \times 10$ | $q^*$(present), $10 \times 42$ | $q^*$(exact[17]) | Percent error, $4 \times 10$ | Percent error, $10 \times 42$ |
|---|---|---|---|---|---|
| 0 | 1.0 | 1.0 | 1.0 | 0.00 | 0.00 |
| 0.1 | 0.9128 | 0.9153 | 0.9157 | −0.32 | −0.04 |
| 0.5 | 0.6979 | 0.7038 | 0.7040 | −0.87 | −0.03 |
| 1 | 0.5484 | 0.5531 | 0.5532 | −0.87 | −0.02 |
| 2 | 0.3874 | 0.3898 | 0.3900 | −0.67 | −0.05 |
| 5 | 0.2078 | 0.2076 | 0.2076 | 0.10 | 0.00 |
| 10 | 0.1173 | 0.1168 | 0.1167 | 0.51 | 0.09 |

**Table 4 Results for the case of single layer of the participating medium**

| | Mode 1 of scattering | | Mode 2 of scattering | |
|---|---|---|---|---|
| $\Re$ | $\kappa$, m$^{-1}$ | $\sigma_s$, m$^{-1}$ | $\kappa$, m$^{-1}$ | $\sigma_s$, m$^{-1}$ |
| | | *Actual values* | | |
| | 0.50 | 1.50 | 0.50 | 1.50 |
| | | *Initial guess* | | |
| | 3.00 | 0.00 | 3.00 | 0.00 |
| | | *Estimated values without perturbation* | | |
| | 0.50 | 1.499 | 0.50 | 1.499 |
| | | *Estimated values with perturbation* | | |
| ±0.5 | 0.496 ± 0.009 | 1.501 ± 0.001 | 0.499 ± 0.013 | 1.499 ± 0.004 |
| ±1.0 | 0.492 ± 0.015 | 1.501 ± 0.003 | 0.497 ± 0.020 | 1.500 ± 0.008 |
| ±1.5 | 0.498 ± 0.032 | 1.499 ± 0.002 | 0.492 ± 0.026 | 1.503 ± 0.010 |
| ±2.0 | 0.495 ± 0.034 | 1.498 ± 0.006 | 0.492 ± 0.040 | 1.505 ± 0.015 |
| ±5.0 | 0.500 ± 0.101 | 1.500 ± 0.012 | 0.546 ± 0.103 | 1.488 ± 0.037 |
| | | *Percent error without perturbation* | | |
| | 0.00 | −0.07 | 0.00 | −0.07 |
| | | *Percent error with perturbation* | | |
| ±0.5 | −0.80 | 0.07 | −0.20 | −0.07 |
| ±1.0 | −1.60 | 0.07 | −0.60 | 0.00 |
| ±1.5 | −0.40 | −0.07 | −1.60 | 0.20 |
| ±2.0 | −1.00 | −0.13 | −1.60 | 0.33 |
| ±5.0 | 0.00 | 0.00 | 9.20 | −0.80 |

### Validation

Because detailed results for the present problem are not available, the results of the present work are benchmarked against the published work for one-dimensional radiative equilibrium between two parallel, isothermal, infinite, diffuse plates enclosing a gray isotropically scattering medium. The results of dimensionless radiative heat flux $q^* = q/\sigma(T_h^4 - T_c^4)$ for various optical thicknesses are compared with the exact results obtained by Heaslet and Warming.[17] The results as obtained from a coarse grid and a fine grid for $0 \le \tau \le 10$ are listed in Table 3. Note that the results predicted by the coarse and fine grids are in very good agreement with the exact solution, and the maximum modulus of error in the case of coarse and fine grids are 0.87 and 0.09%, respectively. This validates the present computational procedure for the pure radiative transfer case.

### Test Cases for the Inverse Problem

*Case 1: Participating Medium Made Up of a Single Layer*

Temperature distribution corresponding to $T_c = 373$ and $T_h = 573$ K, obtained when the direct problem is solved by the use of mode 1 scattering, was taken as the measured temperature. The inverse problem is solved to obtain the parameters that correspond to the actual measured temperature profile, and the values are listed in Table 4. The process of convergence is shown graphically in Fig. 4. In Fig. 4, curves 1 and 2 represent the absorption and scattering coefficients of the participating medium for the case where the measured temperatures are taken without any perturbation. Curves $p1$ and $p2$ show the convergence of parameters by perturbing the measured temperatures using $\Re = \pm 0.5$. Table 4 also gives the variation of the results with respect to changes in $\Re$ and, similarly, results for the use of mode 2 scattering are tabulated.

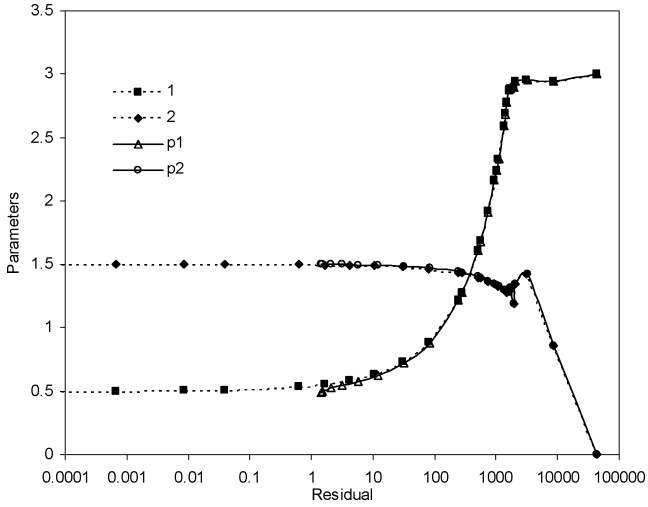


**Fig. 4 Variation of the residual with parameters during the process of convergence to best value for mode1 scattering; absorption and scattering coefficients are represented by 1 and 2, respectively, without perturbation, and, similarly, $p1$ and $p2$ correspond to the case with perturbation level of ±0.5 for a single-layer participating medium.**

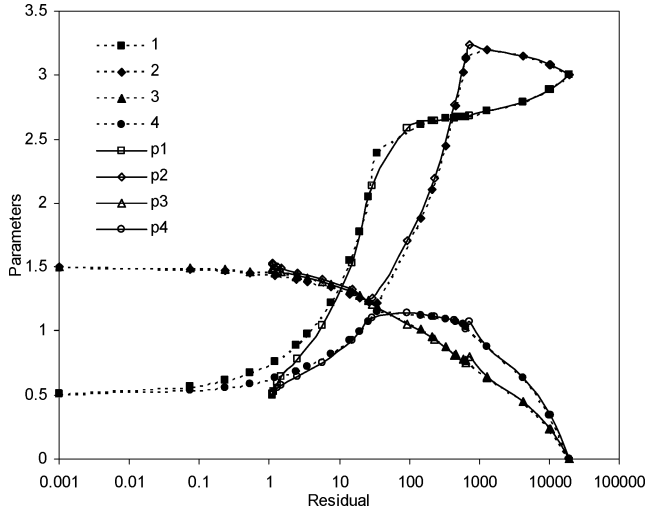


**Fig. 5 Variation of residual with parameters during the process of convergence to best value for mode1 scattering: absorption and scattering coefficients for the bottom and top layers without perturbation are represented by 1, 3, 2, and 4, and, similarly, $p1$, $p3$, $p2$, and $p4$, correspond to the case with perturbation level of ±0.5.**

*Case 2: Participating Medium Made Up of Two Layers*

Here, the problem remains the same as in the preceding case, except that instead of a single layer of participating medium, here we have two layers of the participating medium and each layer is of equal thickness of 0.5 m. Figure 5 shows the graphical convergence of the process starting from the initial guess for the mode 1 of scattering. In Fig. 5, curves 1, 3, 2, and 4 represent the convergence of absorption and scattering coefficients of the bottom and top layers of the participating medium, respectively, for the case where the measured temperatures are taken without any perturbation. Similarly, curves $p1$, $p3$, $p2$, and $p4$ show the convergence of parameters by perturbation of the measured temperatures using $\Re = \pm 0.5$. The results are given in Tables 5 and 6 for the cases of mode 1 and mode 2 scattering, respectively. To further confirm the results, a few runs were also made with the absorption and scattering coefficients of the bottom layer equal to that of the top layer of the participating medium. The results matched exactly with the results obtained by the use of a single layer of the participating medium, for the corresponding absorption and scattering coefficients.

**Table 5 Results for the case of two layers of the participating medium using mode 1 scattering**

| | $\kappa$, m$^{-1}$ | | $\sigma_s$, m$^{-1}$ | |
|---|---|---|---|---|
| $\Re$ | Bottom layer | Top layer | Bottom layer | Top layer |
| | | *Actual values* | | |
| | 0.50 | 1.50 | 1.50 | 0.50 |
| | | *Initial guess* | | |
| | 3.00 | 3.00 | 0.00 | 0.00 |
| | | *Estimated values without perturbation* | | |
| | 0.500 | 1.499 | 1.499 | 0.500 |
| | | *Estimated values with perturbation* | | |
| ±0.5 | $0.502 \pm 0.039$ | $1.494 \pm 0.014$ | $1.499 \pm 0.014$ | $0.505 \pm 0.022$ |
| ±1.0 | $0.534 \pm 0.048$ | $1.494 \pm 0.017$ | $1.492 \pm 0.017$ | $0.516 \pm 0.025$ |
| ±1.5 | $0.469 \pm 0.066$ | $1.522 \pm 0.035$ | $1.512 \pm 0.027$ | $0.470 \pm 0.038$ |
| ±2.0 | $0.498 \pm 0.137$ | $1.525 \pm 0.038$ | $1.500 \pm 0.033$ | $0.486 \pm 0.067$ |
| ±5.0 | $0.556 \pm 0.379$ | $1.462 \pm 0.120$ | $1.511 \pm 0.121$ | $0.517 \pm 0.193$ |
| | | *Percent error without perturbation* | | |
| | 0.00 | −0.06 | −0.06 | 0.00 |
| | | *Percent error with perturbation* | | |
| ±0.5 | 0.40 | −0.40 | −0.07 | 1.00 |
| ±1.0 | 6.80 | −0.40 | −0.53 | 3.20 |
| ±1.5 | −6.20 | 1.47 | 0.80 | −6.00 |
| ±2.0 | −0.40 | 1.67 | 0.00 | −2.80 |
| ±5.0 | 11.20 | −2.53 | 0.73 | 3.40 |

**Table 6 Results for the case of two layers of the participating medium using mode 2 scattering**

| | $\kappa$, m$^{-1}$ | | $\sigma_s$, m$^{-1}$ | |
|---|---|---|---|---|
| $\Re$ | Bottom layer | Top layer | Bottom layer | Top layer |
| | | *Actual values* | | |
| | 0.50 | 1.50 | 1.50 | 0.50 |
| | | *Initial guess* | | |
| | 1.00 | 1.00 | 1.00 | 1.00 |
| | | *Estimated values without perturbation* | | |
| | 0.499 | 1.499 | 1.499 | 0.500 |
| | | *Estimated values with perturbation* | | |
| ±0.5 | $0.501 \pm 0.023$ | $1.511 \pm 0.037$ | $1.503 \pm 0.009$ | $0.494 \pm 0.015$ |
| ±1.0 | $0.507 \pm 0.028$ | $1.550 \pm 0.054$ | $1.508 \pm 0.008$ | $0.488 \pm 0.021$ |
| ±1.5 | $0.496 \pm 0.028$ | $1.446 \pm 0.079$ | $1.485 \pm 0.017$ | $0.526 \pm 0.024$ |
| ±2.0 | $0.501 \pm 0.057$ | $1.499 \pm 0.023$ | $1.513 \pm 0.096$ | $0.506 \pm 0.035$ |
| ±5.0 | $0.540 \pm 0.131$ | $1.463 \pm 0.327$ | $1.485 \pm 0.075$ | $0.497 \pm 0.112$ |
| | | *Percent error without perturbation* | | |
| | −0.20 | −0.07 | −0.07 | 0.00 |
| | | *Percent error with perturbation* | | |
| ±0.5 | 0.20 | 0.73 | 0.20 | −1.20 |
| ±1.0 | 1.40 | 3.33 | 0.53 | −2.4 |
| ±1.5 | −0.80 | −3.60 | −1.00 | 5.20 |
| ±2.0 | 0.20 | −0.07 | 0.87 | 1.20 |
| ±5.0 | 8.00 | −2.47 | −1.00 | −0.60 |

For each perturbation level, 10 different sets of random numbers are generated and each set is added to the measured temperature values to give 10 different sets of input data. These 10 sets of input data for a perturbation level correspond to parameters that are retrieved for each set separately, and their average values with the standard deviation are shown in Tables 4–6. Note from the results that the level of perturbation in the experimental temperature profile affects the values of the estimated parameters more when the parameter itself is small. Also note that the error in the value of the estimated parameter increases with the increase in the level of perturbation, as expected. The results show that this method works well for one and two layers of participating medium, and it is expected to work well for any number of layers of participating media. The process of convergence to the actual values of parameters does not appear to depend on the initial guess, and, in all testing to date, convergence is always to a unique result. The robustness of the procedure followed here was also checked by performance of numerical experiments for a two-layer participating medium, having varying thicknesses for each layer, with a perturbation level up to ±5.0, for the range of $0.2 \le \kappa \le 3.0$, $0.2 \le \sigma_s \le 2.0$, and $0.2 \le L1/L \le 0.8$. Even with a perturbation level of ±5.0, the average values of the retrieved parameters are close to the actual values. The standard deviation, however, is a matter of concern at higher perturbation levels. However, because ultimately we are interested in the average values of the parameter, this problem can be intelligently circumvented by the use of replicate data.

## Conclusions

An inverse method is presented for simultaneous estimation of the absorption and scattering coefficient for both of the layers of a participating medium between two parallel, diffuse, isothermal, infinitely long plates, from the knowledge of a temperature profile available at a set of discrete points. The inverse problem is formulated as an optimization problem and solved by the use of the conjugate gradient method. Noisy input data have been used to test the performance of the proposed method. The results show that the parameters can be estimated with reasonable accuracy, even with small noise in the data. The combination of the finite volume method for the direct problem and the conjugate gradient method for the inverse problem appears to be potent, adequate, and robust for problems of this class. Hence, this procedure can be extended to the inverse radiation analysis for the simultaneous estimation of parameters in a nongray multiple-layer participating medium, which is of engineering interest in many problems.

## References

[1]Howell, J. R., "Thermal Radiation in Participating Media: The Past, the Present, and Some Possible Futures," *Journal of Heat Transfer*, Vol. 110, No. 4(B), 1988, pp. 1220–1229.

[2]McCormick, N. J., "Recent Developments in Inverse Scattering Transport Methods," *Transport Theory and Statistical Physics*, Vol. 13, Nos. 1–2, 1984, pp. 15–28.

[3]McCormick, N. J., "Methods for Solving Inverse Problems for Radiation Transport—An Update," *Transport Theory and Statistical Physics*, Vol. 15, Nos. 6–7, 1986, pp. 759–772.

[4]McCormick, N. J., "Inverse Radiative Transfer Problems: A Review," *Nuclear Science and Engineering*, Vol. 112, No. 3, 1992, pp. 185–198.

[5]Ho, C. H., and Ozisik, M. N., "An Inverse Radiation Problem," *International Journal of Heat and Mass Transfer*, Vol. 32, No. 2, 1989, pp. 335–341.

[6]Yi, H. C., Sanchez, R., and McCormick, N. J., "Bioluminescence Estimation from Ocean In Situ Irradiances," *Applied Optics*, Vol. 31, No. 6, 1992, pp. 822–830.

[7]Li, H. Y., and Ozisik, M. N., "Identification of the Temperature Profile in an Absorbing, Emitting, and Isotropically Scattering Medium by Inverse Analysis," *Journal of Heat Transfer*, Vol. 114, No. 4, 1992, pp. 1060–1063.

[8]Siewart, C. E., "An Inverse Source Problem in Radiative Transfer," *Journal of Quantitative Spectroscopy and Radiative Transfer*, Vol. 50, No. 6, 1993, pp. 603–609.

[9]Siewart, C. E., "A Radiative-Transfer Inverse-Source Problem for a Sphere," *Journal of Quantitative Spectroscopy and Radiative Transfer*, Vol. 52, No. 2, 1994, pp. 157–160.

[10]Li, H. Y., "Estimation of the Temperature Profile in a Cylindrical Medium by Inverse Analysis," *Journal of Quantitative Spectroscopy and Radiative Transfer*, Vol. 52, No. 6, 1994, pp. 755–764.

[11]Li, H. Y., "Inverse Radiation Problem in Two-Dimensional Rectangular Media," *Journal of Thermophysics and Heat Transfer*, Vol. 11, No. 4, 1997, pp. 556–561.

[12]Liu, L. H., "Simultaneous Identification of Temperature Profile and Absorption Coefficient in One-Dimensional Semitransparent Medium by Inverse Radiation Analysis," *International Communications in Heat and Mass Transfer*, Vol. 27, No. 5, 2000, pp. 635–643.

[13]Park, H. M., and Yoon, T. Y., "Solution of the Inverse Radiation Problem Using a Conjugate Gradient Method," *International Journal of Heat and Mass Transfer*, Vol. 43, No. 10, 2000, pp. 1767–1776.

[14]Raithby, G. D., and Chui, E. H., "A Finite-Volume Method for Predicting Radiant Heat Transfer in Enclosures with Participating Media," *Journal of Heat Transfer*, Vol. 112, No. 2, 1990, pp. 415–423.

[15]Siegel, R., and Howell, J. R., "Thermal Radiation Heat Transfer," Taylor and Francis, Washington, DC, 1992, Chaps. 12 and 14.

[16]Fletcher, R., and Reeves, R. M., "Function Minimization by Conjugate Gradients," *The Computer Journal*, Vol. 7, No. 2, 1964, pp. 149–154.

[17]Heaslet, M. A., and Warming, R. F., "Radiative Transport and Wall Temperature Slip in Absorbing Planar Medium," *International Journal of Heat and Mass Transfer*, Vol. 8, No. 7, 1965, pp. 979–994.